# Light scalar mesons in the improved ladder QCD

Toru Umekawa

*Department of Physics, Tokyo Institute of Technology, Meguro, Tokyo 152-8551, Japan*

Kenichi Naito

*Meme Media Laboratory, Graduate School of Engineering, Hokkaido University, Sapporo, Hokkaido 060-8628, Japan*

Makoto Oka

*Department of Physics, Tokyo Institute of Technology, Meguro, Tokyo 152-8551 Japan*

Makoto Takizawa

*Showa Pharmaceutical University, Machida, Tokyo 194-8543, Japan*

The light scalar meson spectrum is studied using the improved ladder QCD with the $U_A(1)$ breaking Kobayashi-Maskawa-'t Hooft interaction by solving the Schwinger-Dyson and Bethe-Salpeter equations. The dynamically generated momentum-dependent quark mass is large enough in the low momentum region to give rise to the spontaneous breaking of chiral symmetry. Due to the large dynamical quark mass, the scalar mesons become the $q\bar{q}$ bound states. Since the parameters have been all fixed to reproduce the light pseudoscalar meson masses and the decay constant, there is no free parameter in the calculation of the scalar mesons. We obtain $M_\sigma = 667$ MeV, $M_{a_0} = 942$ MeV, and $M_{f_0} = 1336$ MeV. They are in good agreement with the observed masses of $\sigma(600)$, $a_0(980)$, and $f_0(1370)$, respectively. We therefore conclude that these states are the members of the light scalar meson nonet. The mass of $K_0^*$ is obtained between that of $a_0$ and $f_0$ and the corresponding state is not observed experimentally. We also find that the strangeness content in the $\sigma$ meson is about 5%.

## I. INTRODUCTION

About three decades ago, quantum chromodynamics (QCD) was conceived as the microscopic theory of the strong interactions. Since then, many aspects of QCD have been studied and QCD has been established as the fundamental theory of the strong interactions. Because of the non-perturbative nature of the low-energy QCD, understanding the low-lying hadron structures from the viewpoint of the quark and gluon degree of freedom is one of the most challenging problems.

The lightest excitation on the QCD vacuum is the pion, which is considered to be a quark and an antiquark bound state in the pseudoscalar channel. Its mass (about 140 MeV) is off-scale light compared with other hadrons such as the $\rho$-meson ($m_\rho \sim 770$ MeV), the spin-flip partner of the pion, and the nucleon ($m_N \sim 940$ MeV), the three-quark bound state. This can be understood by recognizing that the chiral symmetry is spontaneously broken in the QCD vacuum and the pion is the Nambu-Goldstone (NG) boson associated with the dynamical chiral symmetry breaking (DCSB). The DCSB is, therefore, among the most important aspects of low-energy hadron physics. It is believed to be responsible for a large part of the constituent quark masses, which are introduced in the many constituent quark models.

If the QCD Lagrangian has no explicit chiral-symmetry breaking term, the mass of the NG boson associated with the DCSB should be zero. In order to explain the observed mass of the pion, one needs small explicit chiral-symmetry breaking terms, namely current quark mass terms. The NG boson nature of the pion was first studied by Nambu and Jona-Lasinio (NJL) using the schematic model with the four-fermion interaction [1]. Since then, low-energy hadron properties have been widely studied using the NJL-type models [2]. On the other hand, the effects of the explicit breaking of the chiral symmetry on the pion properties have been systematically studied using the effective Lagrangian composed of the pion field. This approach is called the chiral perturbation theory (ChPT) [3]. The success of the ChPT approach supports the importance of the DCSB in low-energy QCD.

When we start looking at the strange quark sector, we encounter another problem. If one assumes that the up, down, and strange quark masses are small compared with the scale of the DCSB, the number of the NG bosons is equal to the dimension of the coset space $U_L(3) \times U_R(3)/U_V(3)$, namely, nine. The ninth heavier pseudoscalar meson is $\eta'$ and its mass is much heavier than the other octet pseudoscalar mesons. Weinberg showed that the mass of $\eta'$ should be less than $\sqrt{3}m_\pi$ if $U_A(1)$ symmetry were not explicitly broken [4]. Thus the $U_A(1)$ symmetry must be broken. The key step to solve this $U_A(1)$ problem was to realize that there is an anomaly in the $U_A(1)$ channel. Namely, the $U_A(1)$ symmetry in the classical theory, i.e., in the action, is broken by quantum effects. In the following year, 't Hooft pointed out the relation between the $U_A(1)$ anomaly and topological gluon configurations of QCD and showed that the interaction of light quarks and instantons breaks the $U_A(1)$ symmetry [5]. He also showed that such an interaction can be represented by a local $2N_f$ quark vertex, which is antisymmetric under flavor exchanges, in the dilute instanton gas approximation.

The effects of the $U_A(1)$ anomaly on the low-energy QCD have been extensively studied in the $1/N_C$ expansion approach [6]. In the $N_C \to \infty$ limit, the $U_A(1)$ anomaly is turned off and then the $\eta$ and $\eta'$ mesons become the ideal mixing states. The flavor component of the $\eta$ is $\frac{1}{2}(u\bar{u} + d\bar{d})$ with $m_\eta(N_C \to \infty) = m_\pi$ and the $\eta'$ meson becomes a pure $s\bar{s}$ state with $m_{\eta'}^2(N_C \to \infty) \simeq 2m_K^2 - m_\pi^2 = (687 \text{ MeV})^2$ [7]. The higher-order effects of the $1/N_C$ expansion give rise to the flavor mixing between the $\eta$ and $\eta'$ mesons and push up the $\eta'$ mass. They were discussed further in the context of the ChPT [8] and a reasonable description of the nonet pseudoscalar mesons was obtained.

The $U_A(1)$ breaking $2N_f$ quark determinant interaction was introduced to the low-energy effective quark models of QCD. The low-lying meson properties have been studied [9–13] using the three-flavor version of the NJL model with the Kobayashi-Maskawa-'t Hooft (KMT) determinant interaction [5,14]. The radiative decays of the $\eta$ meson have been studied in this approach [15] and it was found that these decay widths are reproduced when the $U_A(1)$-breaking interaction is much stronger than the previous studies [9–13]. It is further argued that the $U_A(1)$-breaking interaction gives rise to the spin-spin forces, which are important for light baryons [16–18].

The dynamics of instantons in the multi-instanton vacuum has been studied by many authors, either in the models or in the lattice QCD approach, and the widely accepted picture is that the QCD vacuum consists of small instantons of a size about $1/3$ fm with a density of 1 instanton (or anti-instanton) per fm$^4$ [19]. In the instanton liquid model, the instanton plays a crucial role in understanding not only the $U_A(1)$ anomaly but also the spontaneous breaking of chiral symmetry itself.

Recently, the low-lying scalar mesons, $J^\pi = 0^+$, attracted a lot of attention for two reasons [20]. (i) Experimental evidence for a $\sigma$ ($I = 0$) scalar meson of mass around 600 MeV is overwhelming [21–24]. Especially the decays of heavy mesons show clear peaks in the $\pi\pi$ invariant mass spectrum. Including this rather light isoscalar state, the light scalar mesons show strange mass patterns, i.e., $\sigma(600) - a_0(980) - K_0^*(?) - f_0(980)$, where $K_0^*$ is not confirmed. This pattern cannot be explained as a naive $q\bar{q}$ nonet, because the $I = 1$ $a_0$ states are almost degenerate with the second $I = 0$ state $f_0$, while the first $I = 0$ state $\sigma$ is far below them. (ii) The roles of the scalar mesons in chiral symmetry have been stressed in the context of high temperature and/or density hadronic matter [25]. It is believed that chiral symmetry is restored in the QCD ground state at high temperature (and/or baryon density). Above the critical temperature, $\simeq 170$ MeV, the world is nearly chiral symmetric and we expect that hadrons belong to irreducible representations of chiral symmetry, if we neglect small mixing due to finite quark mass. The pion is no longer a Nambu-Goldstone boson, and has a finite mass and should be degenerate with a scalar meson, i.e., sigma. Another scenario was proposed recently. It is the vector manifestation where the rho meson becomes massless degenerate with a pion as the chiral partner [26]. In order to make the situation clear, we consider that the light scalar mesons are the key particles.

We have studied the effects of the $U_A(1)$ breaking interaction on the low-lying nonet scalar mesons using the extended NJL model, in which the three-flavor NJL model is supplemented with the KMT determinant interaction [27]. Why is the $U_A(1)$ expected to be important in the scalar mesons? It is because the KMT interaction selects out the scalar sector as well as the pseudoscalar mesons and therefore the OZI rule may be broken significantly also in the scalar mesons [28]. We have found that the $U_A(1)$ breaking interaction gives rise to about 150 MeV mass difference between the $\sigma$ and $a_0$ mesons. We have also found that the strangeness content in the $\sigma$ meson is about 15%. The calculated mass of the $I = 1/2$ state ($K_0^*$) was about 200 MeV heavier than that of the $I = 1$ state ($a_0$).

The physics of the light scalar mesons seems to be directly related to the mechanism of the dynamical chiral symmetry breaking (DCSB). In the NJL model, the strong four-quark interaction gives rise to the DCSB and it leads the simple mass relation between the scalar meson mass ($m_S$) and the dynamical quark mass ($M_q$) in the mean-field approximation, i.e., $m_S = 2M_q$ in the chiral limit. In the case of the instanton liquid model, the DCSB is caused by the instanton-induced interaction. The scalar meson masses are rather sensitive to the instanton–anti-instanton interaction. The results in the fully interacting instanton ensemble are $m_\sigma \simeq 0.58$ GeV and $m_{a_0} \simeq 2.05$ GeV [19].

In contrast with the instanton liquid model, the study of the QCD Schwinger-Dyson (SD) equation for the quark propagator in the improved ladder approximation (ILA) has shown that the spontaneous breaking of the chiral symmetry is explained by simply extrapolating the running coupling constant from the perturbative high-energy region to the low-energy region [29]. Then, the Bethe-Salpeter (BS) equation for the $J^{PC} = 0^{-+}$ $q\bar{q}$ channel has been solved in the ILA and the existence of the Nambu-Goldstone pion has been confirmed [30,31]. The numerical predictions of the pion decay constant $f_\pi$ and the quark condensate $\langle \bar{\psi}\psi \rangle$ are rather good. It has been also shown that the BS amplitude shows the correct asymptotic behavior as predicted by the operator product expansion (OPE) in QCD [32]. The masses and decay constants for the lowest-lying scalar, vector, and axial-vector mesons have been evaluated by calculating the two-point correlation functions for the composite operators $\bar{\psi}M\psi$. The obtained values are in reasonable agreement with the observed ones [33].

Then, the current quark mass term has been introduced in the studies of the BS amplitudes in the ILA [34], and reasonable values of the pion mass, the pion decay constant, and the quark condensate have been obtained. It has also been shown that the pion mass square and the pion decay constant are almost proportional to the current quark mass up to the strange quark mass region. The effect of the $U_A(1)$ anomaly is further introduced in the ILA approach by the KMT interaction. The instanton size effects are taken into account by the form factor of the interaction vertices. It guarantees the right asymptotic behavior of the solutions of the SD and BS equations. The properties of the $\eta$ and $\eta'$ mesons have been studied by solving the coupled channel BS equations and the reasonable values of $m_\pi$, $m_\eta$, $m_{\eta'}$, $f_\pi$, and $\langle \bar{q}q \rangle_R$ with a rela-

tively weak flavor mixing interaction (KMT interaction), for which the chiral symmetry breaking is dominantly induced by the soft-gluon exchange interaction [35].

The purpose of this paper is to study the properties of the light scalar meson nonet in the ILA of QCD with the $U_A(1)$ breaking Kobayashi-Maskawa-'t Hooft (KMT) 6-quark flavor determinant interaction. In this approach, the mechanism of the dynamical chiral symmetry breaking is different from the NJL model and the instanton liquid model. It has been shown that the Wilsonian nonperturbative renormalization group equation gives the identical effective fermion mass with that obtained by solving the Schwinger-Dyson equation in the improved ladder approximation [36]. We hope that the present study may shed light on the mechanism of the DCSB in the low-energy QCD. It should be noted here that the parameters have all been fixed in the pseudoscalar meson sector and therefore there is no free parameter in the present study.

There have been many studies of the pion BS amplitude using the effective models of QCD and/or the approximation schemes of QCD [37,38]. The main differences among these studies are the form of the gluon propagator used in the SD and BS equations. Of course, the behavior of the gluon propagator in the asymptotic region is well established and there are no differences. However, the behavior in the infrared region is not well known. The simple infrared cutoff is introduced in the ILA, while in the approach given in [38], the specific form of the infrared gluon propagator is assumed.

Recently, attempts have been made to evaluate enhancement of the gluon propagator (as well as the vertex factor) from quenched lattice QCD data of the quark propagator [39,40]. They found that the gluon propagator is required to have strong enhancement in the soft momentum region so that chiral symmetry is dynamically broken. Although the enhancement patterns vary among the models and parametrizations, they tend to show similar behavior when the solution of the SD equation, i.e., the quark mass function, is con-

cerned. Thus we expect that the results for the mesonic bound state in the BS equation with the effective quark mass function qualitatively agree among the models.

The paper is organized as follows. In Sec. II we explain the Lagrangian we use in the present study and derive the SD equation for the quark propagator and the BS equation for the scalar meson. Section III is devoted to the numerical results. Finally, a summary and concluding remarks are given in Sec. IV.

## II. FORMULATION

In this section, we present the formulation of the improved ladder QCD with KMT interaction. The rainbow approximation is applied to the SD equation for the quark propagator and to the BS equation for the pseudoscalar and scalar mesons. Since the derivations of the SD equation and the BS equation for the pseudoscalar mesons have been given in Ref. [35], here we present only the results.

### A. Improved ladder QCD with KMT interaction

The improved ladder QCD is based on the ladder approximation, which is improved by replacing the coupling constant by the running coupling constant. We employ the rainbow approximation of the SD equation for the quark propagator and the ladder approximation of the BS equation for the quark-antiquark bound states. Improvement is made by the use of the running coupling constant according to the Higashijima-Miransky [29,30,33] method. The Higashijima-Miransky formulation has been justified by the Wilsonian non-perturbative renormalization group (NRG) method. Local potential approximation in the NRG equation gives the SD equation for a single quark and the BS equation for bound states. By employing the gauge coupling constant improved perturbatively, the NRG equation leads to the improved ladder SD equation with the Higashijima-Miransky prescription [36].

Under this approximation, the gluon exchange interaction $\mathcal{L}_{\mathrm{GE}}$ becomes

$$\mathcal{L}_{\mathrm{GE}} = -\frac{1}{2}\int_{pp'qq'} i\bar{g}^2\left(\left(\frac{p-q'}{2}\right)^2,\left(\frac{q-p'}{2}\right)^2\right)D^{\mu\nu}\left(\frac{p+p'}{2}-\frac{q+q'}{2}\right)\bar{\psi}(p)\gamma_\mu T^a\psi(p')\bar{\psi}(q)\gamma_\nu T^a\psi(q')e^{-i(p+p'+q+q')x}, \quad (1)$$

where we use an abbreviation $\int_p = \int[d^4p/(2\pi)^4]$. For the gluon propagator, we employ the Landau gauge,

$$iD^{\mu\nu}(k) = \left(g^{\mu\nu} - \frac{k^\mu k^\nu}{k^2}\right)\frac{-1}{k^2} \quad (2)$$

and the Higashijima-Miransky-type running coupling constant $\bar{g}^2$ defined as follows [29,30,33]:

$$\bar{g}^2(p_E^2,q_E^2) = \theta(p_E^2-q_E^2)g^2(p_E^2) + \theta(q_E^2-p_E^2)g^2(q_E^2) \quad (3)$$

with

$$g^2(p_E^2) = \begin{cases} \dfrac{1}{\beta_0}\dfrac{1}{1+t} & \text{for } t_{\mathrm{IF}} \leqslant t \\[2.5ex] \dfrac{1}{2\beta_0}\dfrac{3t_{\mathrm{IF}}-t_0+2-\dfrac{(t-t_0)^2}{t_{\mathrm{IF}}-t_0}}{(1+t_{\mathrm{IF}})^2} & \text{for } t_0 \leqslant t \leqslant t_{\mathrm{IF}} \\[2.5ex] \dfrac{1}{2\beta_0}\dfrac{3t_{\mathrm{IF}}-t_0+2}{(1+t_{\mathrm{IF}})^2} & \text{for } t \leqslant t_0, \end{cases}$$

$$(4)$$

$$t = \ln \frac{p_E^2}{\Lambda_{QCD}^2} - 1, \tag{5}$$

$$\beta_0 = \frac{1}{(4\pi)^2} \frac{11N_C - 2N_f}{3}. \tag{6}$$

Here, $p_E$ and $q_E$ denote the Euclidean momenta defined by

$$p = (p_0, \vec{p}) \rightarrow p_E = (ip_4, \vec{p}), \tag{7}$$

$$p^2 = p_0^2 - \vec{p}^2 \rightarrow p_E^2 = -p^2 = \vec{p}^2 + p_0^2. \tag{8}$$

In Eq. (4), the infrared cutoff $t_{IF}$ is introduced. Above $t_{IF}$, $g^2(p_E^2)$ develops according to the one-loop solution of the QCD renormalization-group equation, while below $t_0$, $g^2(p_E^2)$ is kept constant. These two regions are connected by a quadratic polynomial so that $g^2(p_E^2)$ becomes a smooth function. Here $N_C$ and $N_f$ are the number of colors and active flavors, respectively. We use $N_C = N_f = 3$ in this study.

The KMT interaction $\mathcal{L}_{KMT}$ is given by

$$\mathcal{L}_{KMT} = -\frac{1}{3} G_D \epsilon^{f_1 f_2 f_3} \epsilon^{g_1 g_2 g_3} \int_{p_1 p_2 p_3 q_1 q_2 q_3} e^{-i(p_1+p_2+p_3+q_1+q_2+q_3)x} w(p_1, p_2, p_3, q_1, q_2, q_3) \{ [\bar{\psi}_{g_1}(p_1) \psi_{f_1}(q_1)] [\bar{\psi}_{g_2}(p_2) \psi_{f_2}(q_2)]$$

$$\times [\bar{\psi}_{g_3}(p_3) \psi_{f_3}(q_3)] + 3[\bar{\psi}_{g_1}(p_1) \psi_{f_1}(q_1)] [\bar{\psi}_{g_2}(p_2) \gamma_5 \psi_{f_2}(q_2)] [\bar{\psi}_{g_3}(p_3) \gamma_5 \psi_{f_3}(q_3)] \}, \tag{9}$$

where $f_1, g_1, \ldots$ are flavor indices, and $\epsilon$ denotes the antisymmetric tensor with $\epsilon^{uds} = 1$ This interaction breaks the $U_A(1)$ symmetry and also mixings of quark flavors. We introduce a weight function

$$w(p_1, \ldots, q_3) = \exp[-\kappa(p_1^2 + \cdots + q_3^2)] \tag{10}$$

so that the KMT interaction is turned off at large momentum region. Then the asymptotic behavior of the ILA is kept consistent with the perturbative QCD. The parameter $\kappa$ is taken as $\kappa = 0.7$ [GeV$^{-2}$]. This value corresponds to the form factor of the instanton of the average size $\rho \sim 1/3$[fm] [35].

### B. Schwinger-Dyson equation

The SD equation in the momentum space is written as

$$iS_F^{-1}(q) - iS_0^{-1}(q) = -C_F \int_p \bar{g}^2(-q^2, -p^2) iD^{\mu\nu}(p-q) \gamma_\mu S_F(p) \gamma_\nu - G_D \int_{p,k} w(-q^2 - p^2 - k^2) \text{tr}^{(DC)}[S_F(p)] \text{tr}^{(DC)}[S_F(k)], \tag{11}$$

where $\text{tr}^{(DC)}$ means the trace of the Dirac and color components and $C_F = (N_C^2 - 1)/2N_C$. Here, the flavor antisymmetrization is assumed in the second term of the right-hand side. This equation is shown diagrammatically in Fig. 1.

Generally, the quark propagator is parametrized as

$$S_F(q) = \frac{i}{\slashed{q} A(q^2) - B(q^2)}. \tag{12}$$

In the Landau gauge, it can be shown that the solution satisfies $A(-q_E^2) = 1$. Then the SD equation becomes the integral equation only of the mass function $B(q^2)$. Our numerical results of the mass function are shown in Fig. 2.
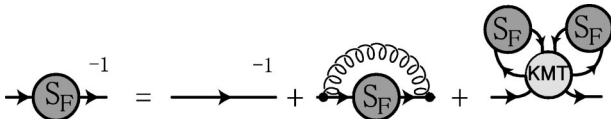
The quark masses are renormalized as



FIG. 1. The Schwinger-Dyson equation.

$$m_q = Z_{m_q}^{-1} m_{qR}, \quad m_s = Z_{m_s}^{-1} m_{sR}, \tag{13}$$

where we take the renormalization condition as

$$\left. \frac{\partial B_q(\mu^2)}{\partial m_{qR}} \right|_{m_{qR}=0} = 1, \tag{14}$$

$$\left. \frac{\partial B_s(\mu^2)}{\partial m_{sR}} \right|_{m_{sR}=0} = 1. \tag{15}$$

We define the quark condensate as follows:

$$\langle \bar{\psi}(0) \psi(0) \rangle = -\int_p \text{tr}[S_F^R(p)] + \int_p \text{tr}[S_F^{\text{pert}}(p)], \tag{16}$$

where

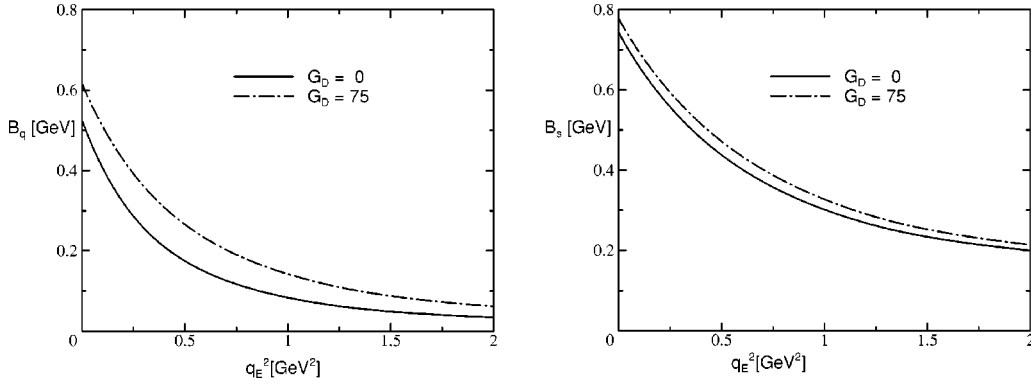$$S_F^R(p) = \frac{i}{\slashed{p} - B(p^2)}, \tag{17}$$

FIG. 2. $q_E^2$ dependences of the mass function of the light ($q$) quark, $B_q$, and the stranger ($s$) quark, $B_s$, for $G_D = 0$ and 75 [GeV$^{-5}$].

$$S_F^{\text{pert}}(p) = \left. \frac{\partial S_F^R(p)}{\partial m_R} \right|_{m_R=0} m_R. \qquad (18)$$

The detail of the renormalization procedure is given in [34].

### C. Bethe-Salpeter equation

To treat the scalar and pseudoscalar mesons as quark-antiquark bound states, we use the homogeneous Bethe-Salpeter equation. The BS equation in momentum space becomes

$$S_F^{-1}(q_+)\chi(q;P)S_F^{-1}(q_-) = -iC_F \int_k \bar{g}^2(-q^2,-k^2)iD^{\mu\nu}(q-k)\gamma_\mu\chi^R(k;P)\gamma_\nu - 2iG_D\int_p\int_k w\left(-p^2-q^2-k^2-\frac{P_B^2}{2}\right)\text{tr}^{(\text{DC})}[S_F^R(p)]$$

$$\times \{\gamma_5\text{tr}^{(\text{DC})}[\gamma_5\chi^R(k;P_B)] + \text{tr}^{(\text{DC})}[\chi^R(k;P_B)]\}, \qquad (19)$$

where $q_\pm = q \pm (P_B/2)$, $\chi(k;P_B)$ denotes the BS amplitude, and $P_B$ is the momentum of the meson. Like the SD equation, the $G_D$ term is antisymmetrized in the flavor space. All the momentum integrals are regularized by the cutoff $\Lambda_{\text{UV}}$, which is chosen as $\Lambda_{\text{UV}} = 100$ [GeV]. Then the results are insensitive to $\Lambda_{\text{UV}}$. This equation is shown diagrammatically in Fig. 3.

For the scalar meson, the BS amplitude can be parametrized in terms of four Dirac structures with appropriate flavor structures,

$$\chi^R(k;P) = 1_C \frac{\lambda^a}{2}\left(\phi_S^a(k;P) + \phi_P^a(k;P)\slashed{k} + \phi_Q^a(k;P)\slashed{P}\right.$$

$$\left. + \phi_T^a(k;P)\frac{1}{2}(\slashed{P}\slashed{k} - \slashed{k}\slashed{P})\right). \qquad (20)$$

The normalization condition of the BS amplitude is given by
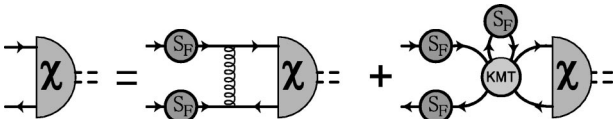
$$i\int_{-q_+^2\leq\Lambda_{\text{UV}}^2,-q_-^2\leq\Lambda_{\text{UV}}^2} \frac{d^4q}{(2\pi)^2}\chi_{n_1m_1}(q;P)\bar{\chi}_{m_2n_2}(q;P)$$

$$\times P^\mu\frac{\partial}{\partial P^\mu}\{S_{F_{n_2n_1}}^{-1}(q_+)S_{F_{m_1m_2}}^{-1}(q_-)\} = -2P^2, \qquad (21)$$

where the indices $m_1, n_1, \ldots$ are combined indices in the color, flavor, and Dirac spaces.

In the numerical computation, we solve the BS equation in the Euclidean momentum region. Then the physical solution, which corresponds to negative $P_E^2$, is obtained by extrapolation from the $P_E^2 > 0$ region. It can be done in the following way. First, we rewrite the Euclidean BS equation in the form

$$\phi_A(q;P_E) = \int_{k_E} M_{AB}(q_E;k_E;P_E)\phi_B(k;P_E), \qquad (22)$$

where $\phi_A$ and $\phi_B$ denote a set of amplitude. This equation should not have a solution at $P_E^2 > 0$ because, if there is one, it is a tachyon solution. Therefore, we instead solve an eigenvalue equation

$$\lambda(P_E^2)\phi_A(q_E;P_E) = \int_{k_E} M_{AB}(q_E;k_E;P_E)\phi_B(k_E;P_E) \qquad (23)$$

for a fixed $P_E^2 > 0$. Then we extrapolate the eigenvalue $\lambda$ to $P_E^2 < 0$ as a function of $P_E^2$ and search for the on-shell point



FIG. 3. The Bethe-Salpeter (BS) equation.

TABLE I. The values of the parameters and the obtained observable quantities.

| $m_{qR}(2[\text{GeV}])$ [MeV] | $m_{sR}(2[\text{GeV}])$ [MeV] | $\Lambda_{\text{QCD}}$ [MeV] | $t_{\text{IF}}$ | $t_0$ | $G_D$ [GeV$^{-5}$] | $\kappa$ [GeV$^{-2}$] |
|---|---|---|---|---|---|---|
| 4.5 | 150 | 600 | 0.204 | −6.89 | 75 | 0.7 |

$\lambda(-M_B^2)=1$. We employ the quadratic function of $P_E^2$ for the extrapolation.

## III. NUMERICAL RESULTS

### A. Parameters

In the present approach, there are seven input parameters: the bare quark mass $m_{q0}$ for the up and down quarks, in which we assume isospin symmetry $m_u=m_d$, the current quark mass $m_{s0}$ for the strange quark, the scale parameter of QCD running coupling constant $\Lambda_{\text{QCD}}$, the infrared cutoff $t_{\text{IF}}$, the smoothness parameter $t_0$, the strength parameter of the KMT $G_D$, and the parameter of the weight function of the KMT $\kappa$. We choose these parameters to reproduce the observables of the pseudoscalar mesons and then we apply them to the scalar mesons.

The quark masses $m_{q0}$, $m_{s0}$ are chosen so that the renormalized masses at the momentum scale $\mu=2$ [GeV] become the $m_{qR}=4.5$ [MeV] and $m_{sR}=150$ [MeV], respectively. The $\kappa$ parameter is taken as $\kappa=0.7$ [GeV$^{-2}$], which corresponds to the instanton of the average size $1/3$ [fm]. The other parameters $\Lambda_{\text{QCD}},t_{\text{IF}},t_0,G_D$ are chosen as the pseudoscalar meson masses $M_\pi,M_\eta,M_{\eta'}$ and the pion decay constant $f_\pi$ are fitted to the experimental values. The parameters that we use are $\Lambda_{\text{QCD}}=600$ [MeV], $t_0=-6.89$, $t_{\text{IF}}=0.204$, and $G_D=75$ [GeV$^{-5}$]. These parameters give $M_\pi=136$ [MeV], $M_\eta=515$ [MeV], $M_{\eta'}=982$ [MeV], and $f_\pi=95$ [MeV]. These are in agreement with experimental values in less than 6% of deviation. Table I summarizes all the values of the parameters.

Although $\Lambda_{\text{QCD}}$ is somewhat larger than the standard value $\Lambda_{\text{QCD}}=100-300$ [MeV], a large $\Lambda_{\text{QCD}}$ is necessary in the ILA to generate the desired dynamical chiral symmetry breaking (D$\chi$SB). It is known that by using the running coupling constant obtained by the higher loop calculation, the smaller $\Lambda_{\text{QCD}}$ gives rise to the correct size of the DCSB. On the other hand, the Wilsonian nonperturbative renormalization group analysis has shown that the effects beyond the ladder approximation also reduce $\Lambda_{\text{QCD}}$ [41].

### B. Solution of the SD equation

The numerical solutions of the SD equation are shown in Fig. 2. The values of the quark condensates and mass function at $P_E^2=0$ are given in Table II.

TABLE II. The values of the mass function at $P_E^2=0$ and the quark condensates.

| $B_q(0)$ | $B_s(0)$ | $-\langle\bar{q}q\rangle_R^{1/3}$ |
|---|---|---|
| 0.616 [GeV] | 0.778 [GeV] | 0.259 [GeV] |

### C. Solution of the BS equation for the scalar mesons

As mentioned above, since the parameters of this approach have been chosen using the observables of the pseudoscalar mesons, the following numerical results of the scalar mesons are parameter-free predictions.

Let us now start the discussion of the solutions of the BS equation. Our numerical results for the scalar mesons are summarized in Table III. The dependence of the mass spectra on the strength of the KMT interaction is shown in Fig. 4.

First, the dependences of the masses of $\sigma$ and $a_0$ on $G_D$ look qualitatively the same as the NJL results shown in [27]. In the NJL calculation, the parameters are chosen so as to reproduce the $M_\pi$ and $f_\pi$ at each $G_D$. In contrast, in the ILA approach we change $G_D$ independently. However, since $M_\pi$ and $f_\pi$ depend weakly on $G_D$, the results of ILA show similar behavior to those of NJL. We note that the mass of $a_0$ grows as $G_D$ increases, while the $\sigma$ mass is almost constant.

The $\sigma$ meson mass is predicted as about 670 [MeV]. This rather small $\sigma$ meson mass is interesting. In the case of the NJL model, the $\sigma$ meson mass is determined to be close to twice the dynamical quark mass. On the other hand, in the ILA approach, the value of the mass function at $q_E^2=0$, $B_q(q_E^2=0)$ is about 616 [MeV], which is comparable to the $\sigma$ meson mass. Recently, Maris calculated the $\sigma$ meson mass in the SD and BS approach with the infrared enhanced gluon propagator [42] and the obtained mass is 671 [MeV]. Although there are such differences, the properties of the physical observables agree in these calculations.

Concerning the $a_0$ meson, we obtain $M_{a_0}=942$ [MeV]. This result is comparable to the experimental value $984.8\pm1.4$ [MeV]. We obtain significant mass splitting between the $\sigma$ and $a_0$, about 275 [MeV]. We conclude that the observed $\sigma-a_0$ mass splitting can be explained as the $U_A(1)$ symmetry breaking effects. Recent study of the light flavor scalar mesons in the instanton liquid model showed a similar result [43].

The obtained mass of $f_0$ is 1336 MeV. We therefore identify this state with $f_0(1370)$ whose T-matrix pole position is

TABLE III. The numerical results of the BS equation.

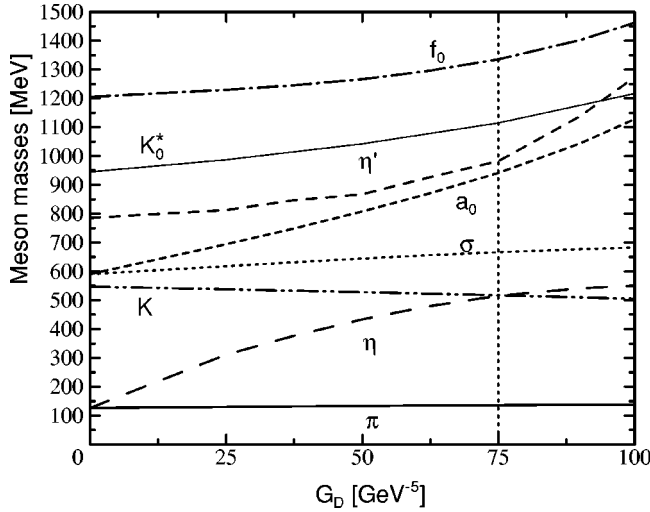| | Mass (MeV) | |
|---|---|---|
| $\pi$ | 136 | $f_\pi=95$ [MeV] |
| $\eta$ | 515 | mixing angle −20.0° |
| $\eta'$ | 982 | mixing angle −26.2° |
| $K$ | 517 | |
| $\sigma$ | 667 | mixing angle −68° |
| $a_0$ | 942 | |
| $f_0$ | 1336 | mixing angle −83.9° |
| $K_0^*$ | 1115 | |

FIG. 4. Dependence of the mass spectrum of the scalar and pseudoscalar meson nonet on the strength of the KMT interaction.



FIG. 5. Extrapolation of the eigenvalue $\lambda$ with respect to $P_E^2$ for $\sigma$, $a_0$, and $f_0$ mesons. The solid line shows the extrapolation of $\sigma$, the dotted line shows the extrapolation of $a_0$, and the dashed line shows the extrapolation of $f_0$.

$(1200-1500)-i(150-250)$ MeV. The calculated mass of $f_0$ is about 400 MeV larger than that of $a_0$. The mixing angle of $f_0$ is $-83.9°$ and it means that this state is close to the flavor octet state. In such a case, the effects of the KMT term on the $f_0$ state are almost the same as that on $a_0$ and therefore the origin of the mass difference between $f_0$ and $a_0$ is considered to be mostly the symmetry breaking effects by the strange quark mass.

The $f_0(980)$ state is observed between $\sigma(600)$ and $f_0(1370)$. From the present study, it seems unlikely that $f_0(980)$ is a simple $q\bar{q}$-bound state. The literature has suggested that $f_0(980)$ may consist of $q^2\bar{q}^2$ [44–47] or may be a $K\bar{K}$ molecular state [48]. Those studies often indicate that the $a_0(980)$ is also a four-quark state. It conflicts with our picture. Further study is necessary to make the situation clearer.

The dependences of the scalar meson spectrum on the strength of $U_A(1)$ breaking interaction are understood as follows. When $G_D=0$, the $\sigma$ meson is an ideal mixing state $(1/\sqrt{2})(u\bar{u}+d\bar{d})$. As the $G_D$ becomes large, the $\sigma$ approaches the flavor singlet state $(1/\sqrt{3})(u\bar{u}+d\bar{d}+s\bar{s})$. The $\sigma$ meson mass seems to become large because of the increase of the strange component. On the other hand, the KMT interaction is attractive for the flavor singlet state, consequently the $\sigma$ meson mass hardly changes. In the case of $a_0$, since the KMT interaction does not induce the flavor mixing, $a_0$ is fixed on the $(1/\sqrt{2})(u\bar{u}+d\bar{d})$ state. As $G_D$ becomes large, the $a_0$ mass increases by the repulsive KMT interaction. As $G_D$ becomes large, the $f_0$ changes from $s\bar{s}$ to $(2/\sqrt{3})(u\bar{u}+d\bar{d}-2s\bar{s})$. The decreasing of the strange component and the repulsive KMT interaction competes. At the small $G_D$, they are balanced and the $f_0$ mass increases at the large $G_D$ where the flavor of the $f_0$ is sufficiently mixed.

There is a shortcoming in the present approach. The solution of the BS equation is obtained at the Euclidean momentum region. To obtain the physical mass and mixing angle, we have to extrapolate the solution from the spacelike to the timelike region. This is carried out by extrapolating the ei-
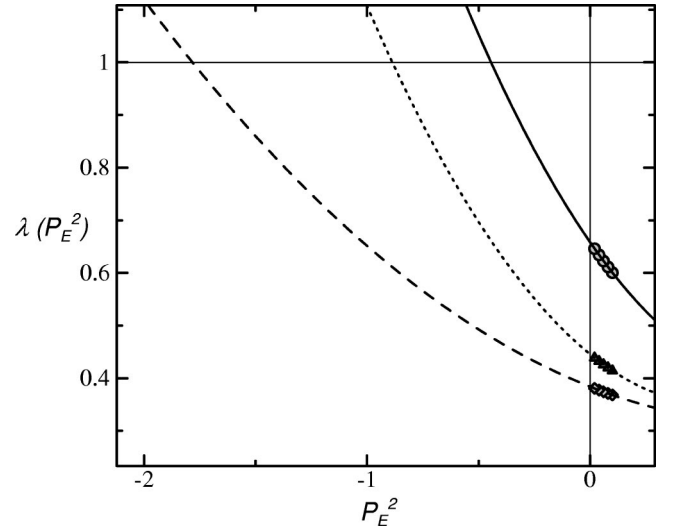
genvalue function $\lambda(P_E^2)$ in Eq. (23) to negative $P_E^2$ until it hits $\lambda(P_E^2)=1$. The graphs of the extrapolation about the masses of $a_0, \sigma, f_0$ are shown in Fig. 5.

We therefore anticipate moderate ambiguity in the extracted masses, especially when the mass is large.

Next, we consider the mixing angles. We introduce the matrix elements $S^8$ and $S^0$, which are defined by

$$S^a = \int d^4x \langle 0|\bar{q}\frac{\lambda^a}{2}q(x)|\text{scalar meson state}\rangle \qquad (24)$$

$$= \text{tr}\left[\bar{\chi}^R(0;P)\frac{\lambda^a}{2}\right]. \qquad (25)$$

Since these $S$ values extract the particular flavor component of $\phi_S$, which is the main component of the BS amplitude at the origin, we employ $S^8$ and $S^0$ to determine the ratio of the octet and the singlet components. Accordingly, we define the mixing angles of the scalar mesons as

$$\tan\theta_\sigma = -\frac{S_0^\sigma}{S_8^\sigma}, \qquad (26)$$

$$\tan\theta_{f_0} = \frac{S_8^{f_0}}{S_0^{f_0}}. \qquad (27)$$

The results are summarized in Table III and Fig. 6.

As $G_D$ increases, the mixing angle moves towards $-90°$, where $\sigma$ becomes the purely flavor singlet state: $(1/\sqrt{3})(u\bar{u}+d\bar{d}+s\bar{s})$. The obtained angle at $G_D=75$ [GeV$^{-5}$] is $-68.0°$ and is slightly smaller than the result of the NJL model, $-77.3°$. This angle corresponds to about 5% mixing of the strangeness component in $\sigma$.
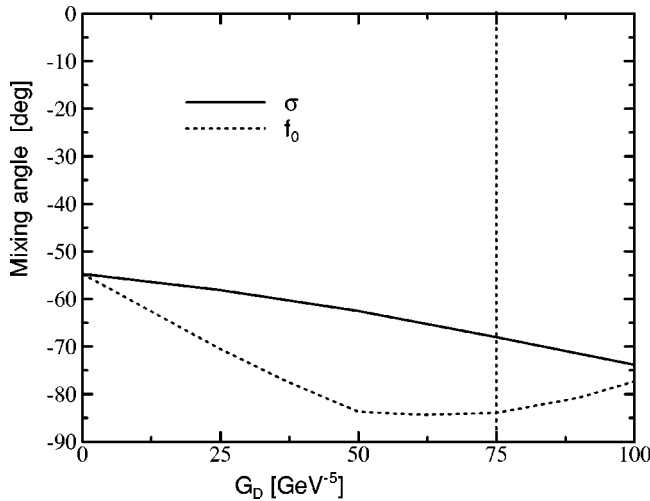
FIG. 6. Dependence of the mixing angle of the $\sigma$ and $f_0$ meson on the strength of the KMT interaction.

### D. Solution of the BS equation for the strange meson

In this section, we discuss the strange scalar meson $K_0^*$. Here we employ an approximation in order to avoid the technical difficulty coming from the ambiguity in defining the center-of-mass coordinate as this meson consists of a strange quark and a nonstrange quark. Instead of treating the asymmetric BS equation, we solve the symmetric BS equation for the quarks of mass $(m_q+m_s)/2=77.25$ [MeV]. We applied this approximation to the kaon and obtained the reasonable kaon mass, $m_K=494$–498 MeV.

The results are summarized in Table III and Fig. 4. The obtained $K_0^*$ mass is 1115 MeV, which is about 173 MeV larger than that of $a_0$ and about 221 MeV smaller than that of $f_0$. If all the $a_0$, $K_0^*$, and $f_0$ states are assumed to be the flavor octet $q\bar{q}$ states, the simple quark model calculation predicts the Gell-Mann-Okubo mass formula. Our results deviate from both the linear mass formula, $3(M_{f_0}-M_{K_0^*})=M_{K_0^*}-M_{a_0}$, and the quadratic mass formula, $3(M_{f_0}^2-M_{K_0^*}^2)=M_{K_0^*}^2-M_{a_0}^2$.

Unfortunately, the corresponding light $I=1/2$ scalar meson is not observed. The observed mass of the $K_0^*(1430)$ is $1412\pm6$ MeV and larger than our result of $M_{f_0}$. It therefore seems to be rather difficult to identify $K_0^*(1430)$ with our $K_0^*$ state. We do not consider $K_0^*(1430)$ as a member of the light scalar nonet states. We hope the reanalysis of the experimental data using the chiral effective model including the effects of the $U_A(1)$ breaking interaction will shed light on the problem of the missing state in the $I=1/2$ scalar channel.

### IV. SUMMARY AND CONCLUSIONS

We have studied the spectrum of the light scalar nonet mesons using the improved ladder approximation (ILA) of QCD with the Kobayashi-Maskawa-'t Hooft (KMT) $U_A(1)$ breaking interaction. We choose parameters to reproduce the masses and decay constants of the pseudoscalar nonet mesons and apply those to the scalar nonet mesons.

The ILA of QCD is an approximation that is consistent with chiral symmetry and consists of the rainbow approximation of the Schwinger-Dyson equation and the ladder approximation of the Bethe-Salpeter equation. Using this approach, we analyze the scalar meson spectrum quantitatively.

We have obtained $M_\sigma=667$ MeV, $M_{a_0}=942$ MeV, and $M_{f_0}=1336$ MeV. Considering the ambiguity due to the extrapolation from the Euclid momentum, they are in good agreement with the observed masses of $\sigma(600)$, $a_0(980)$, and $f_0(1370)$, respectively. We therefore consider that these states are the members of the light scalar meson nonet. This identification is different from the conventional one. The key ingredient is the instanton-induced $U_A(1)$ breaking interaction. It gives rise to the symmetry breaking and flavor mixing effects on the scalar mesons as well as the pseudoscalar mesons.

We have obtained the strangeness content in the $\sigma$ meson of about 5%. This $s\bar{s}$ mixing may be tested, for instance, by analyzing the $\pi\pi$ decays of heavy mesons carefully.

The obtained $K_0^*$ mass is 1115 MeV. The corresponding state is not observed. The observed $K_0^*(1430)$ is heavier than our result of $M_{f_0}$ and therefore we do not include $K_0^*(1430)$ in the light scalar nonet.

It should be noted that the scalar isoscalar state can be mixed with the scalar glueball state. Such an effect is not taken into account here. There is another important effect to be discussed. The light scalar nonet can be generally coupled to the intermediate states composed of two pseudoscalar mesons rather strongly. If the light $q^2\bar{q}^2$ states exist, this coupling effect should be very important. The extension of the Bethe-Salpeter equation to the $q^2\bar{q}^2$ system seems to be rather difficult. One way is to apply the bilocal bosonization technique [49]. Another direction of further study is the extension to the finite temperature and/or density [50]. In the present study, the mass of the $I=1/2$ scalar meson is not reproduced well. In order to make the structure of the light scalar mesons clearer, an analysis of the experimental data using the framework including the $U_A(1)$ breaking interaction is necessary.

[1] Y. Nambu and G. Jona-Lasinio, Phys. Rev. **122**, 345 (1961); **124**, 246 (1961).

[2] For a review, see T. Hatsuda and T. Kunihiro, Phys. Rep. **247**, 221 (1994).

[3] J. Gasser and H. Leutwyler, Ann. Phys. (N.Y.) **158**, 142 (1984).

[4] S. Weinberg, Phys. Rev. D **11**, 3583 (1975).

[5] G. 't Hooft, Phys. Rev. Lett. **37**, 8 (1976); Phys. Rev. D **14**, 3432 (1976).

[6] G. 't Hooft, Nucl. Phys. **B72**, 461 (1974); for a review, see G. A. Christos, Phys. Rep. **116**, 251 (1984).

[7] G. Veneziano, Nucl. Phys. **B159**, 213 (1979).

[8] H. Leutwyler, Nucl. Phys. B (Proc. Suppl.) **64**, 223 (1998).

[9] T. Kunihiro and T. Hatsuda, Phys. Lett. B **206**, 385 (1988); T. Hatsuda and T. Kunihiro, Z. Phys. C **51**, 49 (1991).

[10] V. Bernard, R. L. Jaffe, and U.-G. Meissner, Nucl. Phys. **B308**, 753 (1988).

[11] Y. Kohyama, K. Kubodera, and M. Takizawa, Phys. Lett. B **208**, 165 (1988); M. Takizawa, K. Tsushima, Y. Kohyama, and K. Kubodera, Prog. Theor. Phys. **82**, 481 (1989); Nucl. Phys. **A507**, 611 (1990).

[12] H. Reinhardt and R. Alkofer, Phys. Lett. B **207**, 482 (1988); R. Alkofer and H. Reinhardt, Z. Phys. C **45**, 275 (1989).

[13] S. Klimt, M. Lutz, U. Vogl, and W. Weise, Nucl. Phys. **A516**, 429 (1990).

[14] M. Kobayashi and T. Maskawa, Prog. Theor. Phys. **44**, 1422 (1970); M. Kobayashi, H. Kondo, and T. Maskawa, *ibid.* **45**, 1955 (1971).

[15] M. Takizawa and M. Oka, Phys. Lett. B **359**, 210 (1995); **364**, 249(E) (1995); Y. Nemoto, M. Oka, and M. Takizawa, Phys. Rev. D **54**, 6777 (1996); M. Takizawa, Y. Nemoto, and M. Oka, *ibid.* **55**, 4083 (1997).

[16] E. V. Shuryak and J. L. Rosner, Phys. Lett. B **218**, 72 (1989).

[17] M. Oka and S. Takeuchi, Phys. Rev. Lett. **63**, 1780 (1989); Nucl. Phys. **A524**, 649 (1991); S. Takeuchi and M. Oka, Phys. Rev. Lett. **66**, 1271 (1991).

[18] O. Morimatsu and M. Takizawa, Nucl. Phys. **A554**, 635 (1993).

[19] For a review, see T. Schäfer and E. V. Shuryak, Rev. Mod. Phys. **70**, 323 (1998).

[20] For recent developments, see Proceedings of the workshop "Possible existence of the $\sigma$-meson and its implications to hadron physics," June, 2000 (Yukawa Institute for Theoretical Physics, Kyoto, Japan), KEK-Proceedings 2000-4, Dec. 2000 and Soryushiron Kenkyu (Kyoto) **102** (2001).

[21] Particle Data Group, Phys. Lett. B **592**, 1 (2004), and references therein.

[22] S. Ishida, M. Ishida, H. Takahashi, T. Ishida, K. Takamatsu, and T. Tsuru, Prog. Theor. Phys. **95**, 745 (1996).

[23] K. Igi and K. Hikasa, Phys. Rev. D **59**, 034005 (1999).

[24] R. Kaminski, L. Lesniak, and B. Loiseau, Eur. Phys. J. C **9**, 141 (1999).

[25] T. Hatsuda and T. Kunihiro, Phys. Rev. Lett. **55**, 158 (1985); T. Hatsuda, T. Kunihiro, and H. Shimizu, *ibid.* **82**, 2840 (1999).

[26] M. Harada and C. Sasaki, Phys. Lett. B **537**, 280 (2002); M. Harada, Y. Kim, and M. Rho, Phys. Rev. D **66**, 016003 (2002).

[27] K. Naito, M. Oka, M. Takizawa, and T. Umekawa, Prog. Theor. Phys. **109**, 969 (2003).

[28] V. Dmitrasinovic, Phys. Rev. C **53**, 1383 (1996); Nucl. Phys. **A686**, 379 (2001).

[29] K. Higashijima, Phys. Rev. D **29**, 1228 (1984); V. A. Miransky, Sov. J. Nucl. Phys. **38**, 280 (1984).

[30] K. Aoki, M. Bando, T. Kugo, M. G. Mitchard, and H. Nakatani, Prog. Theor. Phys. **84**, 683 (1990).

[31] K. Naito, K. Yoshida, Y. Nemoto, M. Oka, and M. Takizawa, Phys. Rev. C **59**, 1095 (1999).

[32] K. Aoki, M. Bando, T. Kugo, and M. G. Mitchard, Prog. Theor. Phys. **85**, 355 (1991).

[33] K. Aoki, T. Kugo, and M. G. Mitchard, Phys. Lett. B **266**, 467 (1991).

[34] K. Naito, K. Yoshida, Y. Nemoto, M. Oka, and M. Takizawa, Phys. Rev. C **59**, 1722 (1999).

[35] K. Naito, Y. Nemoto, M. Takizawa, K. Yoshida, and M. Oka, Phys. Rev. C **61**, 065201 (2000).

[36] K. Aoki, K. Morikawa, J. Sumi, H. Terao, and M. Tomoyose, Phys. Rev. D **61**, 045008 (2000).

[37] For a review, see C. D. Roberts and A. G. Williams, Prog. Part. Nucl. Phys. **33**, 477 (1994), and references therein.

[38] P. Maris and C. D. Roberts, Int. J. Mod. Phys. E **12**, 297 (2003).

[39] H. Iida, M. Oka, and H. Suganuma, hep-ph/0312328.

[40] M. S. Bhagwat, M. A. Pichowsky, C. D. Roberts, and P. C. Tandy, Phys. Rev. C **68**, 015203 (2003).

[41] K. Aoki, K. Takagi, H. Terao, and M. Tomoyose, Prog. Theor. Phys. **103**, 815 (2000).

[42] P. Maris, Few-Body Syst. **32**, 41 (2002).

[43] T. Schäfer, Phys. Rev. D **68**, 114017 (2003).

[44] R. L. Jaffe, Phys. Rev. D **15**, 267 (1987).

[45] M. Alford and R. L. Jaffe, Nucl. Phys. **B578**, 367 (2000).

[46] D. Black, A. H. Fariborz, F. Sannino, and J. Schechter, Phys. Rev. D **59**, 074026 (1999).

[47] F. E. Close and N. A. Tornqvist, J. Phys. G **28**, R249 (2002).

[48] J. Weistein and N. Isgur, Phys. Rev. D **41**, 2236 (1990).

[49] C. D. Roberts, R. T. Cahill, M. E. Savoir, and N. Iannella, Phys. Rev. D **49**, 125 (1994).

[50] P. Maris, C. D. Roberts, S. M. Schmidt, and P. C. Tandy, Phys. Rev. C **63**, 025202 (2001).